

# A STUDY OF THE EFFECTS OF LOADING AMPLITUDE AND INDUCED STRESS RATIO ON FATIGUE LIFE OF A NODULAR GRAPHITE CAST IRON STRUCTURE UNDERGOING MULTI-AXIAL PROPORTIONAL CYCLIC LOADING

ADNAN D. MOHAMMED<sup>1</sup> & MAHMOUD KACHIT<sup>2</sup>

<sup>1</sup>Department of Mechanical Engineering, Faculty of Engineering, Philadelphia University, Amman, Jordan

<sup>2</sup>MATIES Laboratories, INSA, Lyon, France

## ABSTRACT

*The influence of loading conditions on fatigue life and stress concentration, on ferritic nodular graphite cast iron material, undergoing multi-axial proportional cyclic loading, is investigated experimentally and numerically. The studies are conducted under a controlled maximum amplitude stress (induced Von Mises stress) of 158 Mpa which is close to the fatigue limit of the studied material. Good agreements are reported between numerical and experimental results. It is found that fatigue life and Von Mises stress concentration depend strongly on cyclic loading amplitude ratio 'R'. Fatigue life is less for proportional loading than for simple torsion or simple axial loading. The ultimate number of cycles, in the studied interval of 'R' (-1 to +1), increases in a linear fashion. It has a minimum value at R equals to -1. This effect is directly related to the maximum Von Mises stress. The latter increases in a linear fashion as R increases from -1 to +1, and exhibits a maximum value at R equals to +1. Also, it is found that fatigue life and Von Mises stress are highly dependent on the induced stress ratio ( $\sigma/\tau$ ). Von Mises stress increases as stress ratio increases. In a reverse manner, fatigue life increases slowly as the ratio  $\sigma/\tau$  increases. This result concludes the strong effect, on fatigue life, of the presence of the axial load within the multi-axial cyclic loading. In fact, axial loading favors the mode I crack which propagates rapidly perpendicularly to the axis of axial loading.*

**KEYWORDS:** Fatigue Life, Ferritic Nodular Graphite Cast Iron, Multi-Axial Loading, Von Mises Stress

**Received:** Apr 16, 2018; **Accepted:** May 07, 2018; **Published:** Jul 07, 2018; **Paper Id.:** IJMPERDAUG201843

## 1. INTRODUCTION

Multi axial fatigue has been studied for a number of years, and recent reviews of the subject show that the research has been concentrated exclusively on proportional loading, i.e. when the applied stresses or strains are maintained in strict proportion throughout the loading cycle. The fatigue life of a material for proportional stresses can be related to crack orientation and the mean value of Von Mises stress. Under proportional states of stress, principal directions are fixed in the space; then also the critical planes are the same at any instant, i.e. the shear stress always has the same direction. Therefore, the Von Mises stress has a physical meaning of the shear stress on a specific plane [1].

### 1.1. Effect of Stress Ratio

The effect of stress ratio has been studied by several authors. The studies have been especially concentrated on FCD700 nodular cast iron. For FCD700 nodular cast iron Endo [2] has concluded that the direction

of a non-propagating crack is approximately normal to the principal stress ( $\sigma_1$ ), regardless of combined stress ratio ( $\tau/\sigma$ ) as illustrated in figure 1. Under a stress slightly higher than the fatigue limit, and when a crack is propagated in a direction normal to  $\sigma_1$ , failure of the specimen occurs.

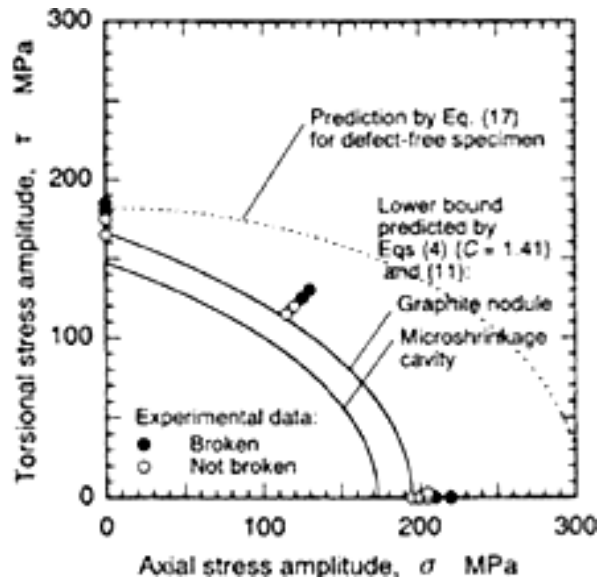


**Figure 1: Comparison between Predicted and Experimental Results for Smooth Nodular Cast Iron Specimens [2]**

In smooth FCD700 specimens, no mode II non-propagating crack was observed at the torsional fatigue limit. Many of the cracks initiated at graphite nodules are in direction of about  $\pm 45^\circ$  to specimen axis [2 & 3]. The  $0^\circ$  or  $\pm 90^\circ$  shear planes mode II nonpropagating cracks were observed in the matrix remote from nodules. The fatigue limit appears to be sufficiently high to nucleate mode II cracks by slip repetitions in the matrix structure and may be why the coexistence of both modes I and mode II non-propagating cracks was observed. In the case of FCD700, the reduction in torsional fatigue strength due to graphite nodules is so large that mode II non-propagating cracks cannot be developed in the matrix [2 & 4].

Because failure in nodular cast iron is controlled by the nucleation and growth of small cracks from inclusions and pores, the second principal stress influences the fatigue strength [5]. Crack driving force near a notch is greater in the case of  $\lambda = -1$  as compared to  $\lambda = 0$ , where  $\lambda$  is the ratio of second to the first principal stresses as illustrated in figure 2. In materials where the fatigue limit strength is controlled by the propagation/no propagation of cracks nucleating at individual small holes or inclusions, it may be expected that the biaxial fatigue limit is higher than that for uniaxial fatigue.

The effect of biaxial stress on Mode I crack growth for AISI316 stainless steel was reported by Gary et al. [5]. At low stresses, the effect of the transverse stress is small with the biaxial tension ( $\lambda = 1$ ) having the lowest growth rate. This may be related to the slightly smaller plastic zone size for this type of loading. The difference between the growth rates increases as the stress levels increases. Only when the nominal stress approaches the yield strength more significant differences in growth rates are reported by above-mentioned authors.

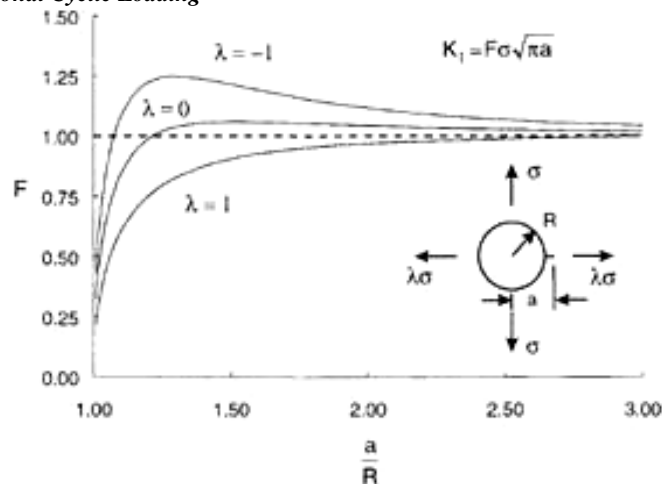


**Figure 2: Stress Intensity Factors for Cracks Initiating at a Hole**

Stress ratio  $\lambda$  takes a maximum value equals to zero regardless of the stress state. Therefore, the fatigue limit is reduced for biaxial stress ratios less than zero but is not necessarily increased for biaxial stress ratios greater than zero. Nodular cast irons are an example of materials that normally fail under cyclic loadings in a brittle fashion. Failure in this case, is often initiated from shrinkage of pores or other casting defects [5].

## 1.2. Crack Orientation

Materials subjected to fatigue loading can be classified into three types according to the cracking behavior [6]. Some materials display shear cracking where fatigue cracks are observed on the material plane of maximum shear amplitude and some materials exhibit tensile cracking where cracks are initiated on the plane of maximum normal stress. Other materials display a mixed cracking behavior where cracks are initiated on the maximum normal planes for tension-compression loading but on the maximum shear plane under pure shear loading. Many materials display mixed cracking behavior, and few, such as stainless steel and aluminum alloys, exhibit tensile cracking behavior [6 & 7]. Very few materials display shear cracking behavior [8].

Fatigue cracks in nodular iron specimens nucleated and propagated on maximum principal stress planes [5, 9 & 10]. Cracks for torsion or tensile loading showed some tortuosity as the crack linked up numerous microstructural features as shown in figure 3, [7]. However, the crack direction is fairly well defined. During equi-biaxial loading, the cracks grew generally in the plane normal to the hoop stress, but in comparison to the torsion or tensile cracks, there is significantly more branching and tortuosity. The Mode I crack driving force was thus nearly equal in all directions. Small cracks in C45 initiate on both  $0^\circ$  and  $90^\circ$  planes for torsion only loading. This is a well-documented phenomenon for ductile metals. Crack growth along the specimen surface is via Mode II crack growth and into the depth of the material by Mode III growth. After shear cracks reach a length of several hundred microns, crack branching along  $\pm 45^\circ$  planes occurs. For near-fatigue limit testing, the crack branching occurs rather late in the total life of the material. Cracks produced by uniaxial tension fatigue are similar for both C45 and nodular cast iron [11], i.e. initiation and propagation is macroscopically always normal to the direction of maximum principal stress (figure 4). For this reason, it is very difficult to distinguish between shear and tensile dominated materials based only on axial tension fatigue loading.

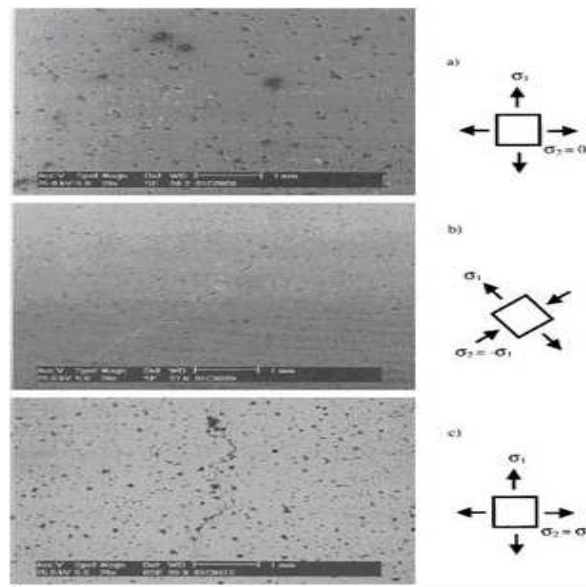


**Figure 3: Fatigue Cracks during: (a) Axial Tension, (b) Torsion, (c) Equi-Biaxial Tension loading for FCD700**

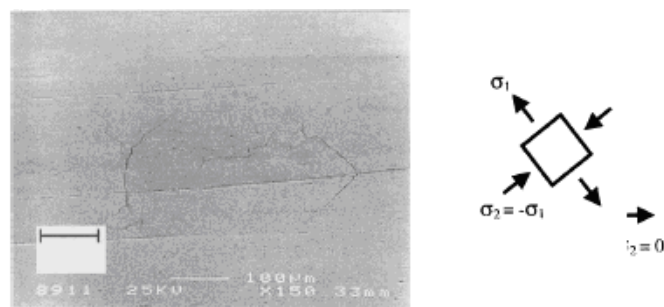


**Figure 4: Fatigue Cracks during Torsion of C45 for Low Carbon Steel**

The objective of this research is to study the influences of type of proportional cyclic loading (axial, torsion and axial – torsional), loading amplitude ratio ‘R’, (at a constant induced maximum stress) and the ratio of axial to torsional stress ( $\sigma/\tau$ ) on the resulting maximum value of Von Mises stress and fatigue life. To achieve this goal it was decided to work on a ferritic spherical graphite cast iron (GS) under a controlled induced maximum Von Mises stress. For this chosen material, the mechanisms of initiation and propagation of cracks under uni-axial cyclic loading are now well understood. These GS irons have the advantage of containing initiation sites of graphite nodules, which are spherical and can be regarded as defects models. In addition, the volume fraction of nodules is about 15%, these initiation sites are numerous and uniformly distributed within the material, thus satisfying a statistical study of initiation.

## 2. EXPERIMENTAL INVESTIGATIONS

Fatigue tests were conducted at MATEIS laboratory – INSA -Lyon-France. These tests were performed under proportional multi-axial cyclic loading (axial – torsional) with a controlled maximum stress using servo-controlled hydraulic testing machine shown in figure 5. The machine was designed to perform tension-compression and torsion tests simultaneously. Crack orientation was investigated after the occurrence of the failure of specimens using Scanning Electronic Microscope (SEM). The specimens used in this study were fabricated from ferritic spherical graphite cast iron (GS). The material is chemically analyzed, and the chemical composition is displayed in Table 1.



**Figure 5: Fatigue Test Machine, Control Unit, and Test Specimen**

**Table 1: Chemical Composition (Mass Percentage) of Tested Material**

Element	C	Si	Mn	S	P	Mg
(m%)	3.4	2.60	0.19	0.005	0.011	0.05

The mechanical properties, (shown in table 2), of the tested material, were obtained using monotonic tensile test machine (CTIF - Central Technical Interception Facility). The elastic modulus was obtained by the method of resonance of a bar (calculating module from the natural frequencies of vibration of the bar). The yield strength at 0.2% strain, the stress at rupture and elongation at fracture are obtained from Figure 6. The latter displays the results for two specimens.

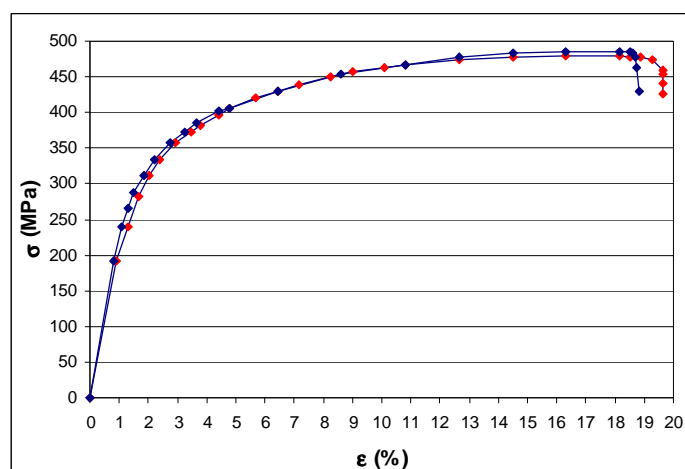


**Figure 6: Tensile Test Curves**

**Table 2: Mechanical Properties of Tested Material**

E (GPa)	$\sigma_{0.2}$ (MPa)	$\sigma_r$ (MPa)	A (%)
168	270	400	20

The specimen, (machined from a cast bar), used in the experimental investigation is cylindrical in shape with a gage length of 25 mm, and a diameter of 6 mm. The geometry and dimensions of the specimen are shown in figure 7. Polishing of specimen was made, longitudinally, on the gage length to provide a flat narrow band (0.5×7mm) which allows good OM and SEM images of cracks.

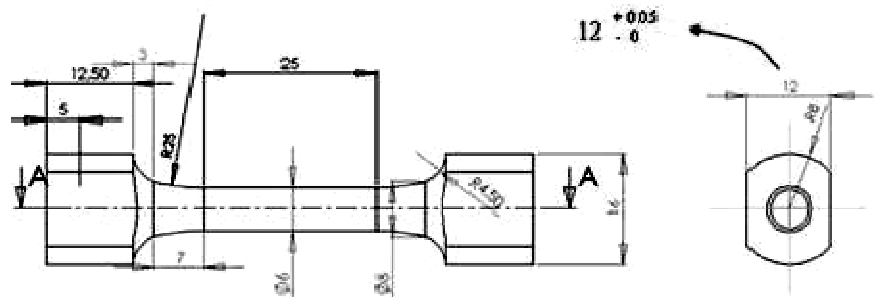


**Figure 7: Geometry and Dimensions of the Test Specimen**

The multi-axial fatigue tests were conducted at room temperature under a controlled maximum stress. A proportional multi-axial (axial – torsional) sinusoidal signal was imposed at a frequency of 10Hz. Simple axial and torsional cyclic loadings tests were conducted for comparison. The effects of cyclic loading amplitude ratio ‘R’, (between the values -1 and +1), and the stress ratio (axial to torsional stress ( $\sigma/\tau$ )), on fatigue life and resulting Von Mises stresses of the tested specimens were investigated.

The crack orientation at the matrix and at the graphite nodules, after the occurrence of fracture of specimens, was studied using Optical Microscope OM and SEM.

### 3. FINITE ELEMENTS MODEL

A Finite Element model for a cylindrical bar, (fixed at one end and free at the other end), was created using Ansys-15 FEM program (Figure 8). Dimensions and material properties are similar to those described in the previous section. The unloaded fixed end was given a horn shape to prevent unwanted stress concentration. Axial, torsional and proportional multi-axial fatigue tests were performed numerically using a controlled maximum stress of amplitude of about 158 MPa. The cyclic loadings were applied at the free end of the cylindrical bar as shown in figure 8. The effects of cyclic loadings amplitude ratio ‘R’, (between the values -1 and +1), and the stress ratio (axial to torsional stress ( $\sigma/\tau$ )), on fatigue life and resulting Von Mises stress of the loaded model were investigated.

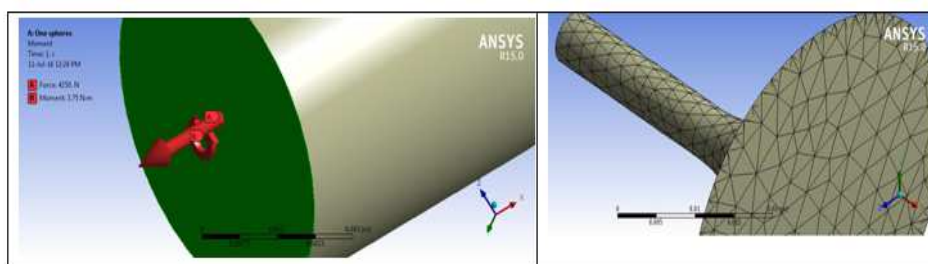


**Figure 8: Configuration of Finite Elements Model**

## 4. RESULTS

### 4.1 Experimental Results

The experimental results of fatigue life were obtained as averages of three tests. The number of cycles at fracture was chosen to correspond to the number of cycles when the specimen is physically broken. Results of fatigue life (ultimate number of cycles (NR)) are displayed in figure 9 as a function of cyclic loading amplitude ratio ‘R’ for three cyclic types of loading; Axial loading, torsional loading, and axial-torsional loading. As clearly demonstrated in the figure, fatigue life is maximum for torsional loading and minimum for multiaxial loading regardless of the value of R. The fatigue life is



shortened by nearly 200,000 cycles for multiaxial loading relative to that of torsional cyclic loading. Fatigue life (NR) value decreases, in approximately linear manner, as the value of  $R$  changes from 1 to -1 for all types of loading.

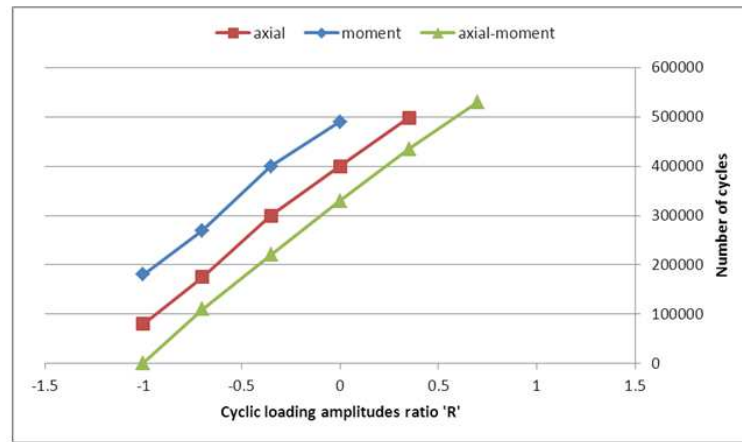


**Figure 9: Ultimate Number of Cycles in Function of Loading Conditions**

Graphite nodules were usual origins of microcracks initiation in GS iron. To understand the cracking behaviors for the three types of loadings studied, a study of cracks orientation was conducted using OM and SEM observations after the occurrence of specimen's rupture.

For torsional loading, the rupture of the surface has the features of static torsion loading, i.e. cracks initiate and propagate at nodules at  $\pm 45^\circ$  in form of a cross (X) relative to the specimen axis (figure 10.c). Many cracks were frequently observed in the matrix, they initiate and propagate at about  $0^\circ$  and  $90^\circ$  relative to the specimen axis (figure 10-a & b). These matrix cracks initiate at localized plastic strain zones characterized by the presence of horizontally oriented (at  $0^\circ$ ) slip microbands. These  $0^\circ$  oriented microbands was developing, during cycling, and reaching, in the final phase of cycling, to about  $30\mu\text{m}$  in length and exhibiting  $5\mu\text{m}$  as an inter-distance. They cause the intrusion-extrusion phenomena which increase the stress concentration at the intrusion bottom and give birth to crack.  $0^\circ$  and  $90^\circ$  oriented cracks are initiated and propagated longitudinally and perpendicularly at slip microbands respectively.  $90^\circ$  oriented cracks are initiated at the locally deformed zone/matrix interface (figure 10.a). Some of  $90^\circ$  oriented cracks are Intergranular cracks initiated and propagated at the boundary of two differently deformed adjacent grains (figure 10-b), where the stress is normally higher and more complex. In this case, the microbands seem to be longitudinally cut (impeded) at the boundary grain, so they grow freely in length on the other side during cycling. Generally, the intergranular cracks are of  $90^\circ$  oriented cracks type; while transgranular cracks are of  $0^\circ$  oriented cracks one.

For axial loading, Mode I cracks initiate at graphite nodules at  $0^\circ$  (figure 10-d). For Axial-Torsional loading, cracks initiate at graphite nodules at  $+33^\circ$  and  $-66^\circ$  (figure 10-e).

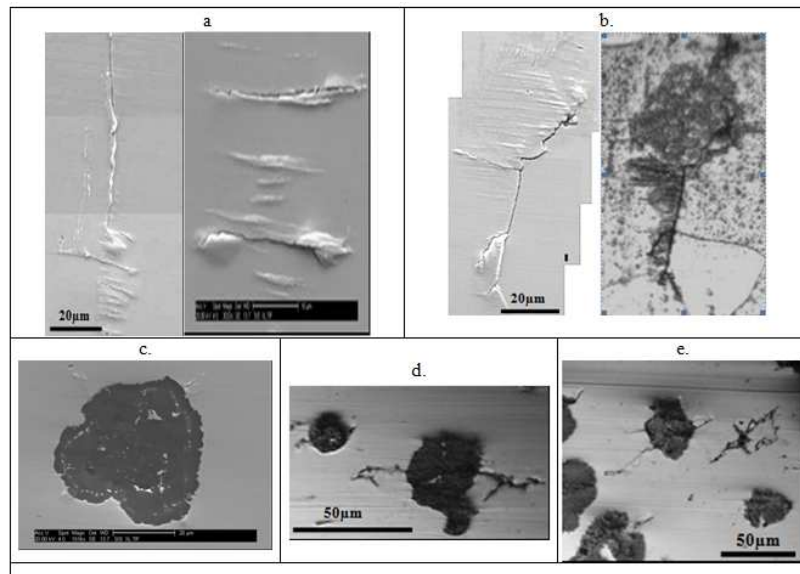


**Figure 10: (a) 0° and 90° Oriented Matrix Cracks in Torsional Loading, (b) Intergranulated Crack in Torsional Loading, (c) ±45° Oriented Cracks at Nodules in Torsional Loading, (d) 0° Oriented Nodule Cracks in Axial Loading, (e) +33° and -66° Oriented Nodule Cracks in Axial-Torsional Loading**

#### 4.2. Finite Elements Results

Fatigue life and Von Mises stresses of the FE model under axial, torsional and multi-axial cyclic loadings environments were studied. The following two effects on fatigue life were considered in the current study: the effect of the ratio (R) and the effect of stress ratio ( $\sigma/\tau$ )

##### 4.2.1. The Effect of the Ratio 'R'

The effect of loadings amplitude ratio 'R' on fatigue life and maximum Von Mises stress concentration of the model were studied for the three types of studied cyclic loadings (axial, torsional, and axial - torsional) using the fatigue module in the finite element package. Figure 11 shows the effect of 'R' on the maximum value of Von Mises stress. Von Mises stress, for all studied loadings, increases from a minimum value ( $VM = 0$ ) at  $R=1$  to a maximum value at  $R= -1$  (symmetric mode). The increase in the value of Von Mises stress is more clearly seen for multi-axial loading than those for pure torsional or pure axial loadings.

The behavior of fatigue life curves is inversely similar to VM ones (figure 12). The contribution of the axial load in uni- and multi-axial loadings increase the maximum Von Mises stress and consequently reduces the fatigue life. This result confirms the strong effect of the axial loading in the proportional multi-axial cyclic loading. Indeed, the torsional loading generates 0° and 90° oriented matrix non-propagating cracks, so increasing the fatigue life. The axial loading increases the driving force of 0° cracking in mode I and hence contributing to the reduction of the fatigue life. In fact, axial loading causes 0° oriented matrix cracks undergoing a maximum cracking force due to the homogeneity of stresses distribution across the section of the specimens. Fatigue life is considerably shortened when one of multiaxial the cyclic loads is an axial load.



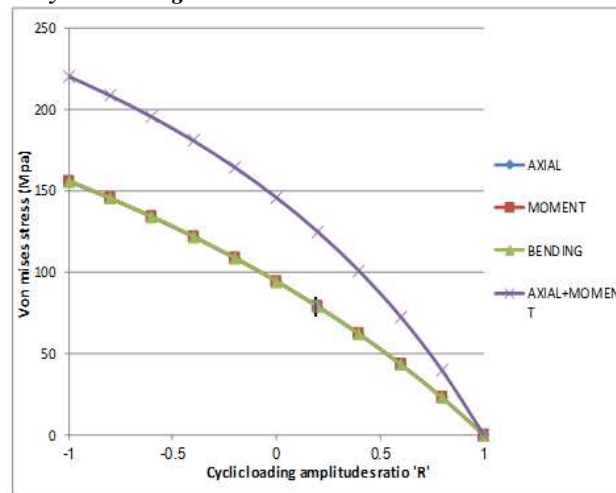


**Figure 11: Effect of R on Mean Von Mises Stress**

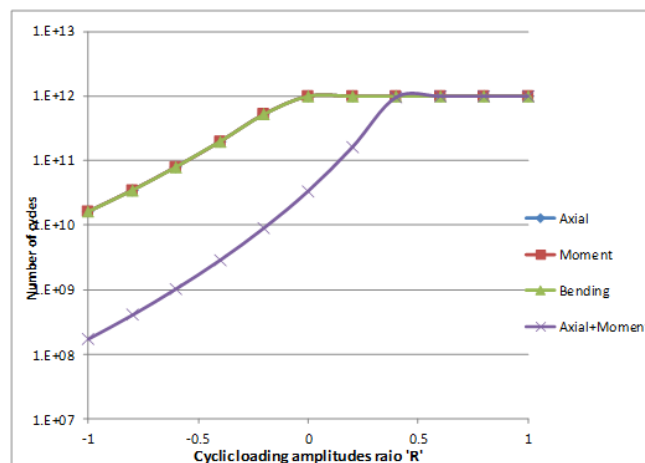


**Figure 12: Effect of R on Mean Fatigue Life**

The fatigue life behavior obtained by finite element method is similar to that obtained experimentally (figure 9). The values obtained experimentally are always less than those obtained numerically. This is may be due to different experimental factors such asspecimen's surface roughness and mounting conditions ... etc.

#### 4.2.2. The Effect of Stress Ratio ( $\sigma/\tau$ )

The aim here is to study the sensitivity of the maximum Von Mises stress and the fatigue life to the type of load (axial, torsional and axial – torsional). The effect of the ratio of induced normal stress to induced shear stress ( $\sigma/\tau$ ) on fatigue life was investigated using finite element method. The ratio was evaluated by, firstly, changing induced  $\sigma$  and keeping  $\tau$  as constant ( $\sigma/\tau$ ), then, by changing  $\tau$  and keeping  $\sigma$  as constant ( $\tau/\sigma$ ). Fatigue life and Von Mises stress curves were plotted versus the stress ratio in figures 13 and 14 respectively.

When the ratio  $\sigma/\tau$  equals 1.0, the maximum Von Mises equivalent stress has a minimum value (nearly 210MPa) and the fatigue life has a maximum value (almost  $3 \times 10^8$  cycles) (figure 13). When  $\sigma/\tau$  is increased by increasing  $\sigma$ , maximum Von Mises stress increases rapidly to reach an approximate value of 540MPa when the crack occurs. At this point, the ratio  $\sigma/\tau$  is 1.7 and fatigue life reached the value of  $10^4$  cycles as shown in figure 14.

When  $\tau/\sigma$  equals to 1.0, maximum Von Mises equivalent stress has always a minimum value (nearly 210MPa) and fatigue life has a maximum value (almost  $3 \times 10^8$  cycles). When  $\tau/\sigma$  is increased by increasing  $\tau$ , the maximum Von Mises equivalent stress increases slowly, and almost linearly from 210MPa up to 550MPa (when the crack is occurred). Here, the value of  $\tau/\sigma$  is 2.5 and fatigue life has the value of  $2 \times 10^3$  cycles.

At  $\sigma/\tau = \tau/\sigma = 1.7$ , fatigue life is larger by a factor of approximately 100 when increasing  $\tau$  than increasing  $\sigma$ . Therefore, increasing the intensity of axial load has more influence on shortening the fatigue life than increasing the intensity torsional load. Also, the sensitivity of fatigue life to axial loading is highly marked.

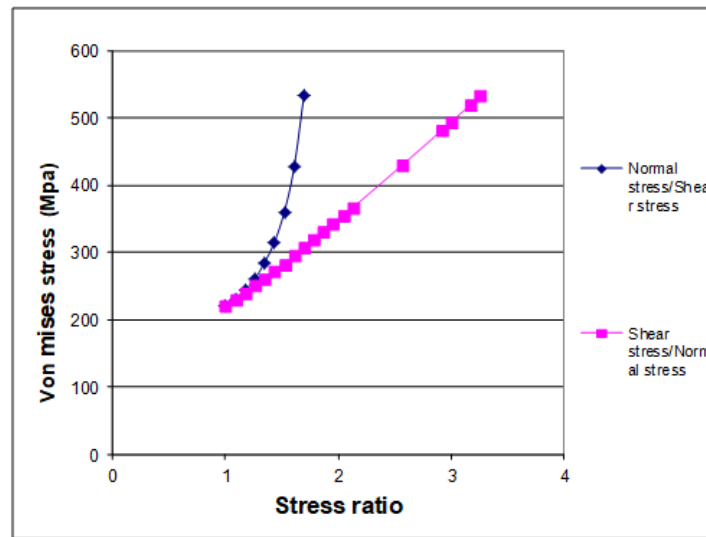


Figure 13: Effect of Stress Ratio on Maximum Von Mises Stress

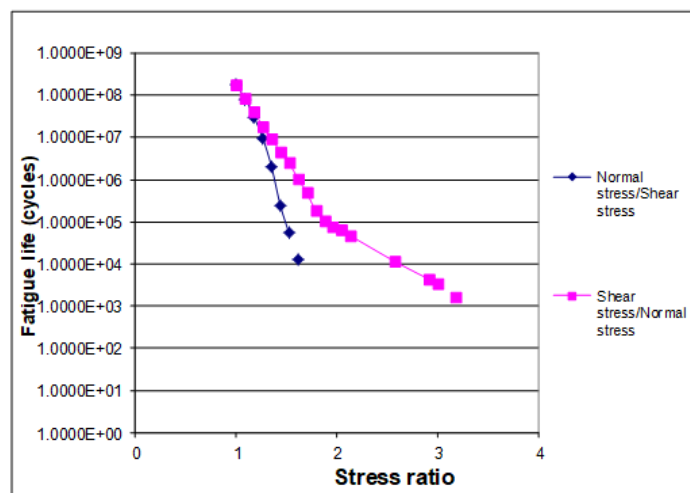


Figure 14: Effect of Induced Stress Ratio on Fatigue Life

## 5. DISCUSSION OF RESULTS

As mentioned earlier, ferrite ductile iron was studied experimentally and numerically under three different loading environments; axial, torsion and axial-torsional loading. Theoretical backgrounds for the effects of cyclic loading amplitude ratio 'R' ratio and induced stress ratio  $\sigma/\tau$  on the resulting Von Mises stress and crack orientation are described as follows:

The principal directions are those where the only stresses are normal stresses. These stresses are called principal stresses and are found from the original stresses expressed in the x and y directions as:

$$\sigma_{1,2} = \frac{\sigma_x + \sigma_y}{2} \pm \sqrt{\left(\frac{\sigma_x - \sigma_y}{2}\right)^2 + \tau_{xy}^2} \quad (1)$$

The maximum shear stress is equal to one-half the difference between the two principal stresses,

$$\tau_{\max} = \sqrt{\left(\frac{\sigma_x - \sigma_y}{2}\right)^2 + \tau_{xy}^2} = \frac{\sigma_1 - \sigma_2}{2} \quad (2)$$

For general plan stress (present case), where  $\sigma_3 = \sigma_{31} = \sigma_{32} = 0$ , Von Mises stress equation can be simplified and written as:

$$\sigma_{VM} = \sqrt{\sigma_{11}^2 - \sigma_{11}\sigma_{22} + \sigma_{22}^2 + 3\sigma_{12}^2} \quad (3)$$

The results obtained from the present investigation show that NR decreases linearly with R in the intervals  $R = -1$  to  $+1$ . For all types of employed loadings, when R changes from  $+1$  to  $-1$ , at a constant maximum fatigue stress, principal stresses, and Von Mises stress increase (according to the equations 2 and 3), and, consequently, fatigue life is reduced. The high value of first principal stress  $\sigma_1$  increases the magnitude of driving force of cracking and therefore shortening the fatigue life.

The Fatigue life is displayed as a function of the type of load (see figures 9 & 12). Whatever the value of R, fatigue life has the lowest values for combined axial-torsional loading. For tension-compression axial cyclic loading, NR is higher compared to that obtained under multi-axial loading. Fatigue life reaches the highest value when the loading is torsional.

As reported from experimental investigation of the present study, specimens that were subjected to uniaxial tension load has failed at noticeably lower NR value compared to those subjected to the torsional load. This is in a good agreement with the results obtained numerically. For this type of loading, the transformation to the maximum principal stress direction and Mohr's circle are illustrated in figure 15. The first principal stress  $\sigma_1$  is responsible for the initiation of crack (at graphite nodule) and propagation of  $0^\circ$  mode I (propagated at the principal maximum stress plane (see figure 10.d).

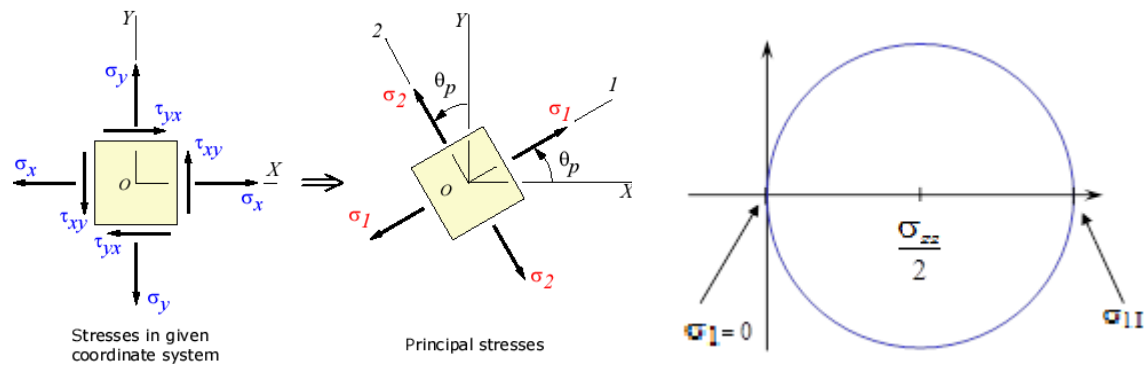


**Figure 15: Transformation of the Maximum Principal Stress Directions and Mohr's Circle for Axial Loading**

This type of propagated cracks increases the speed of cracking and shortens the fatigue life compared with the case when the load is torsional. Here, cracks are of  $0^\circ$  and  $90^\circ$  non-propagating type (see figure 10.a). Under torsional loading,  $\pm 45^\circ$  cracks are initiated at principal maximum stress plane (at nodule graphite) as shown in figure 10.c. This is in accordance with the maximum shear stress direction and Mohr's circle illustrated in figure 16.

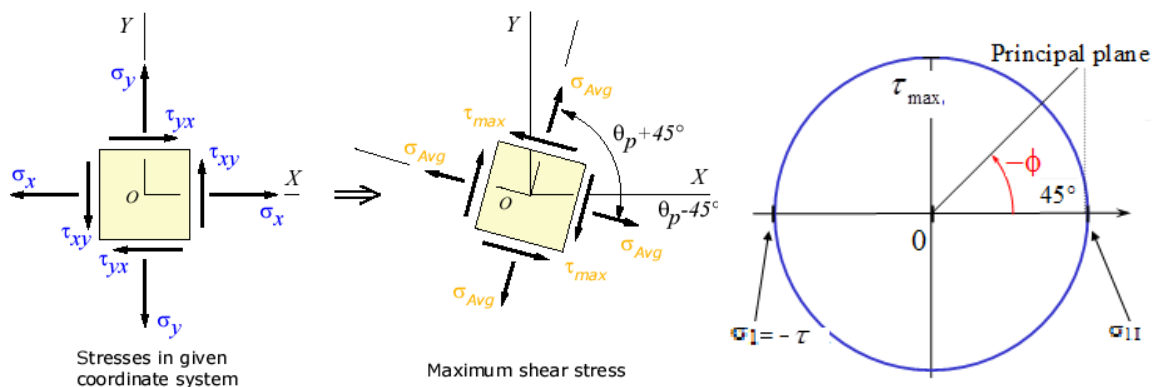


**Figure 16: Transformation of the Maximum Shear Stress Directions and Mohr's Circle for Torsional Loading**

For multi-axial (axial – torsional) proportional cyclic loading,  $\sigma_1$  and  $\sigma_{VM}$  have the highest values, and consequently, the driving force of cracking is here the most important, and therefore fatigue life is the shortest. For this type of loadings, cracks are initiated at principal maximum stress plane oriented at  $+33^\circ$  and  $-66^\circ$  from the specimens axis as shown in figure 10.e. This is confirmed by Mohr's circle shown in figure 17.

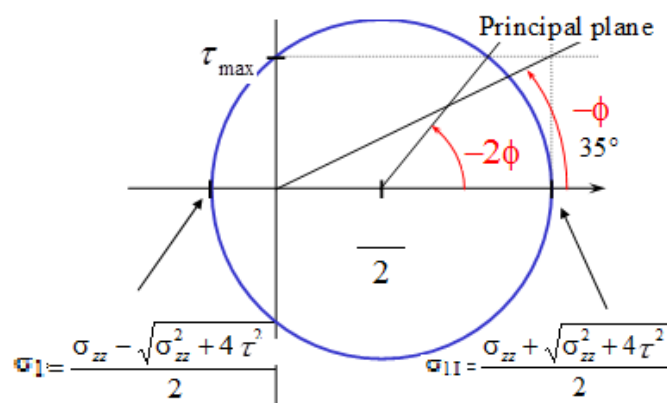


**Figure 17: Mohr's Circle for Axial-Torsional Loading**

Even when the applied loading is predominantly torsional, damage in nodular iron is observed to occur along maximum principal stress planes rather than shear planes. The driving force of cracks emanating from defects in axial-torsional loading is significantly more than that for tension or torsion. It would be expected that the fatigue limit under axial-torsional loading would be lower than for either uniaxial tension or pure torsion. Finite element results obtained for the model that is subjected to axial-torsional loading showed that failure has occurred at noticeably lower fatigue life (NR) compared with those obtained under simple torsion or simple axial loadings.

## 5.2. Effect of Induced Stress Ratio

The numerical FEM results demonstrate the strong negative effect of axial cyclic loading on fatigue life. Fatigue life is highly affected by axial loading than by torsional loading.

In nodular graphite cast iron, it is reported that the direction of a non-propagating crack is approximately normal to the principal stress,  $\sigma_1$ , regardless the values of combined stress ratio,  $\tau/\sigma$ . Under a stress,  $\sigma_1$ , slightly higher than the fatigue limit, a crack which is propagated in a direction normal to  $\sigma_1$  resulted in the failure of the specimen and hence reducing fatigue life.

The studied material displays a mixed cracking behavior where cracks are initiated on the maximum normal planes for tension-compression loading but on the maximum shear plane under pure shear loading (ref. figure 10.d). The short crack model is based on mixed-mode crack growth taking into the account mode I and mode II crack deformation [4]. Under pure tension loading, the short crack model always predicts mode I crack growth occurring on planes of maximum normal stress. Under pure shear loading, the short crack model predicts shear cracking for low cycle fatigue (ref. figure 10.a) and shear transformed to tensile cracking for high cycle fatigue (see figure 10.c). Consequently, under axial – tension loading this study predicts mode I crack growth occurring on planes of maximum normal stress oriented at  $+33^\circ$  and  $-67^\circ$  (see figure 10.e). For this loading, the axial component increased the maximum principal stress, consequently, the driving force of cracking is increased, and the fatigue life is reduced. Whereas, the torsion component causes matrix non-propagating mode II to crack and do not contribute, significantly, to the reduction of fatigue life.

## 6. CONCLUSIONS

The influence of the condition of solicitation on the maximum value of Von Mises stress and fatigue life was investigated on the cylindrical bar of ferritic nodular graphite cast iron subjected to multi-axial, proportional cyclic loading (axial-torsional having different loading amplitude ratio "R" and different induced stress ratio  $\sigma/\tau$ ). Finite element method and experimental investigation demonstrated that:

- Fatigue life is relatively small for multi-axial loading in comparison to those for simple torsion or simple axial loading. This is due to the high value of concentrated Von Mises stress and driving force of mode I cracking resulted from multi-axial loading.
- Fatigue life increases, in a linear fashion, as the stress amplitude ratio (R) increases. It exhibits a minimum value at  $R = -1$ . This effect is directly related to the maximum value of concentrated Von Mises Stress and consequently to the driving force of mode I cracking.
- Fatigue life under multi-axial loading is highly affected by the variation of the magnitude of axial loading and less sensitive to the variation in torsion loading.

- Therefore, it can be recommended that the weight of the structure or mechanical plant (generally generates an axial load) should be minimized to reduce the axial loading component. At the same time, the torsional component of loading can be, consequently increased in order to permit maximum torque transmission.

## REFERENCES

1. C. Braccesi, F. Cianetti, G. Lori and D. Pioli, *An Equivalent Uniaxial Stress Process For Fatigue Life Estimation of Mechanical Components Under Multi-axial Stress Conditions*, *International Journal of Fatigue*, Vol. 30, pp. 1479–1497, 2008.
2. M. Endo, *The multi-axial fatigue strength of specimens containing small defects*, *Biaxial/Multi-axial Fatigue and Fracture*, Andrea Carpinteri, Manuel de Freitas and Andrea Spagnoli, Vol. 31, 1<sup>st</sup> edition, pp. 243-264, 2003.
3. D. Roo, and P. Clement, *Influence des petits défauts sur la résistance en fatigue d'une fonte GS ferritique*. *Fonderie Fondeur d'Aujourd'hui*, no 64, pp. 30-37, 1987.
4. K. Tokaji, and T. Ogama, *Fatigue life Distribution And Its Simulation in Spheroidal Graphite Cast Irons*, *Materials Science Research International*, Vol. 2, no.1, pp. 39-45, 1996.
5. G. B. Marquis and P. Karjalainen-Roikonen, *Long-life Multi-axial Fatigue of a Nodular Graphite Cast Iron*, *Biaxial/Multi-axial Matigue and Fracture*, Andrea Carpinteri, Manuel de Freitas and Andrea Spagnoli, Vol. 31, 1<sup>st</sup> edition, pp. 105-122, 2003.
6. Y. Jiang, O. Hertel and M. Vormwald, *An Experimental Evaluation of Three Critical Plane Multi-Axial Fatigue Criteria*, *International Journal of Fatigue*, Vol. 29, pp. 1490–1502, 2007.
7. M.J. Dong, G.K. Hu, A. Diboine, D. Moulin and C. Prioul, *Damage modelling in Nodular Cast Iron*, *Journal de Physique*, IV, Colloque C7, , Vol. 3, p. 643, 1993
8. C. Verdu, J. Adrien and J.Y. Buffière, *Three-Dimensional Shape of The Early Stages of Fatigue Cracks Nucleated in Nodular Cast Iron*, *Materials Science and Engineering (A)*, Vol. 483, pp. 402–405, 2008.
9. Ghosh, Sugato. "Rydberg Atom Transition with Quantum Optic Ions with Amplitude Modulation with Response of Pulse Wave."
10. A. Suzuki, Y. Hirose, Z. Yajima, and K. Tanaka, *Fatigue Crack Nucleation and Growth Behavior of Ductile Cast Iron*, *Soc. Strength Fract. Mater.*, Vol. 27, pp. 9-21, 1993.
11. P. Clement, J.P. Angeli, and A. Pineau, "Short crack behaviour in nodular cast iron. *Fatigue Engineering Materials Structures*, 1984, Vol. 7, no. 4, pp. 251-265, 1984.
12. Dierickx P., *Etude de la microstructure et des mécanismes d'endommagement de fontes G.S. ductiles : influence des traitements thermiques de ferritisation (in French)*, Ph.D. dissertation, INSA de Lyon, 1996.